Zhongbo Liu,[1] Jose Cordoba-Chacon,[2,3] Rhonda D. Kineman,[2,3] Bruce N. Cronstein,[4] Radhika Muzumdar,[5] Zhenwei Gong,[5] Haim Werner,[6] and Shoshana Yakar[1]

Growth Hormone Control of Hepatic Lipid Metabolism

In humans, low levels of growth hormone (GH) and its mediator, IGF-1, associate with hepatic lipid accumulation. In mice, congenital liver-specific ablation of the GH receptor (GHR) results in reductions in circulating IGF-1 and hepatic steatosis, associated with systemic insulin resistance. Due to the intricate relationship between GH and IGF-1, the relative contribution of each hormone to the development of hepatic steatosis is unclear. Our goal was to dissect the mechanisms by which hepatic GH resistance leads to steatosis and overall insulin resistance, independent of IGF-1. We have generated a combined mouse model with liver-specific ablation of GHR in which we restored liver IGF-1 expression via the hepatic IGF-1 transgene. We found that liver GHR ablation leads to increases in lipid uptake, de novo lipogenesis, hyperinsulinemia, and hyperglycemia accompanied with severe insulin resistance and increased body adiposity and serum lipids. Restoration of IGF-1 improved overall insulin sensitivity and lipid profile in serum and reduced body adiposity, but was insufficient to protect against steatosis-induced hepatic inflammation or oxidative stress. We conclude that the impaired metabolism in states of GH resistance results from direct actions of GH on lipid uptake and de novo lipogenesis, whereas its actions on extrahepatic tissues are mediated by IGF-1.

According to Browning et al. (1), nonalcoholic fatty liver disease (NAFLD) affects almost one-third of the adult population in North America. Low levels of growth hormone (GH) in the general population associate with NAFLD (2).

Multi–single nucleotide polymorphism analyses of genome-wide association study have revealed 18 single nucleotide polymorphisms in the GH pathway that relate to the development and progression of NAFLD (3). Also, patients with GH receptor (GHR) loss of function (Laron syndrome) exhibit NAFLD (4). Likewise, cessation of GH treatment in GH-deficient (GHD) children after achieving adult height leads to development of NAFLD and dyslipidemia in 29% of patients surveyed 10 years after therapy (2). Importantly, reductions in circulating GH (2,5) or its mediator, IGF-1 (6–8), associate with NAFLD even after adjusting to BMI (9). Obese patients manifest GH resistance and can show declines in GH (10,11) that may be as low as those observed in GHD subjects (12,13). GH therapy reduces fat in young men with abdominal obesity (14), patients with primary GHD (5,15,16), and hepatosteatosis in patients with HIV lipodystrophy (17). In contrast, humans treated with the GHR antagonist (pegvisomant and somatostatin analogs) to control for endogenous GH levels (18) show increased hepatic triglyceride (TG) content.

In rodents, diet-induced fatty liver associates with reduced circulating GH (19,20) and reduced signal transducer and activator of transcription-5 (STAT5) phosphorylation in response to GH stimulation (21). Liver-specific deletion of GHR in mice results in a marked decrease in serum IGF-1 levels, significant increases in fat mass and serum lipids, and severe hepatic steatosis associated with systemic insulin resistance (22). A similar metabolic phenotype is observed in mice with liver-specific disruption of the GHR mediators Janus kinase-2 (JAK2) (23) or STAT5 (24).

[1]Department of Basic Science & Craniofacial Biology, David B. Kriser Dental Center, NYU College of Dentistry, New York, NY
[2]Research and Development, Jesse Brown VA Medical Center, Chicago, IL
[3]Department of Medicine, Section of Endocrinology, Diabetes and Metabolism, University of Illinois at Chicago, Chicago, IL
[4]Department of Medicine, NYU School of Medicine, New York, NY
[5]Division of Pediatric Endocrinology, Diabetes and Metabolism Consultation, Children's Hospital of Pittsburgh of UPMC, University of Pittsburgh School of Medicine, Pittsburgh, PA
[6]Department of Human Molecular Genetics and Biochemistry, The Sackler School of Medicine, Tel Aviv University, Ramat Aviv, Israel

Corresponding author: Shoshana Yakar, sy1007@nyu.edu.

GH treatment in mice reduced diet-induced hepatosteatosis (21,25), and overexpression of a GHR antagonist increased hepatic steatosis (26).

Clearly, clinical and experimental data indicate that reductions in circulating GH levels or hepatic response to GH are a typical component of NAFLD. On the basis of the above evidence, a clinical trial is currently underway to test the effectiveness of GH treatment in reducing hepatic lipid content in patients with NAFLD (NCT02217345).

Addressing the molecular mechanisms by which GH regulates hepatic lipid metabolism is challenging; models with ablation of GHR action in liver show significantly reduced serum IGF-1 levels accompanied with high GH levels that affect carbohydrate and lipid metabolism in extrahepatic tissues. Thus, the direct roles of hepatic GH in lipid and carbohydrate metabolism are not known. We hypothesized that hepatic GHR regulates lipid metabolism independent of IGF-1 and that reductions in hepatic GHR signaling are not merely a consequence of NAFLD but a contributor to hepatic lipid accumulation in NAFLD. To address our hypothesis, we generated a mouse model with hepatic ablation of the GHR (Li-GHRKO) and restored IGF-1 gene expression via hepatic IGF-1 transgene (HIT). The Li-GHRKO-HIT mice show normal levels of serum IGF-1 and exhibit hepatic GH resistance.

RESEARCH DESIGN AND METHODS

Animals
The generations of HIT mice (27) and floxed ghr mice (28) were previously described. Gene inactivation of the ghr in liver was achieved by the cre/lox-P system, as described by us previously (29). All mice were in the C57BL/6J genetic background. Weaned mice were allocated randomly into cages separated according to their sex. Mice were housed two to five animals per cage in a facility with 12-h light/dark cycles and free access to food/water. The different analyses were performed in male mice at the indicated ages.

All animal procedures were approved by the Institutional Animal Care and Use Committee of the NYU School of Medicine (assurance number A3435–01; U.S. Department of Agriculture license no. 465).

Serum Hormones
Serum/plasma were collected via orbital bleeding immediately after euthanasia with CO_2 between 8 and 10 A.M. Hormones were measured by ELISA: GH (EZRMGH-45K; Millipore), IGF-1 (22-IG1MS-E01; ALPCO), leptin (EZRL-83K; Millipore), insulin (NC9440604; Mercodia), IGF-1 binding protein-3 (IGFBP-3; EMIGFBP3; Thermo Fisher Scientific), cytokines (K152A0H-1; Meso Scale Discovery), serum IGFBP-1 (CL0383; Cell Applications, Inc.), and IGFBP-2 (IRKTAH5375; Innovative Research, Inc.). Serum acid labile subunit (ALS) levels were determined by Western immunoblotting (AF1436; R&D Systems).

Serum and Tissue Lipids
Free fatty acids (FFAs) were measured using calorimetric assay (11383175001; Roche). Liver TG content was assessed following chloroform-methanol extraction and quantified using the TG reagent (T7531; Pointe Scientific). Serum samples were sent to ANTECH Diagnostics (New Hyde Park, NY) for cholesterol measurements.

Tissue FA Composition
Tissue FA composition was determined by gas chromatography/mass spectrometry (GC/MS) after lipid extraction, as described previously (30).

Liver Glycogen Content
Liver glycogen content was measured using colorimetric assay (glycogen kit NC0294986; Cayman Chemical).

Liver Enzymes
Serum samples were sent to ANTECH Diagnostics for measurements of aspartate transaminase (AST), alanine transaminase (ALT), and alkaline phosphatase.

Blood Glucose Measurements, Insulin, Glucose, and Pyruvate Tolerance Tests
Mice were injected with 0.5 U/kg insulin, 2 mg/g glucose, or 2 g/kg sodium pyruvate (S8636; Sigma-Aldrich) for tolerance tests. Blood glucose levels were measured using a glucometer (Elite; Bayer, Mishawaka, IN). Insulin tolerance was measured in fed mice, glucose tolerance in 8-h–fasted mice, and pyruvate tolerance in 15-h–fasted mice.

Lipid Peroxidation
Thiobarbituric acid–reactive substances were measured using a commercial kit (10009055; Cayman Chemical).

Protein Oxidation
Carbonylated proteins were detected using an OxiSelect Protein Carbonyl Spectrophotometric assay (STA-315; Cell Biolabs, Inc.).

Gene Expression
RNA was extracted using TRIzol (Invitrogen, Carlsbad, CA) or RNeasy Plus (74134; Qiagen), reverse-transcribed (18080-051; Life Technologies), and subjected to real-time PCR using SYBR master mix (4385612; Life Technologies/Applied Biosystems). Transcript levels were corrected to 18S. The primer sequences are presented in Supplementary Table 2.

Western Immunoblot Assay
Proteins were extracted using CHAPS buffer (1.25% CHAPS; 28300; Thermo Fisher Scientific) with protease inhibitor cocktail (04693132001; Roche), separated on 4–20% SDS-PAGE (NP0335; Life Technologies), and transferred to nitrocellulose membranes (170-4158; Bio-Rad). Antibodies used were anti-F4/80 (MCA497R; AbD Serotec), anti–insulin receptor (IR; sc-711; Santa Cruz Biotechnology), actin (4970; Cell Signaling Technology), and secondary antibodies (7074; Cell Signaling Technology).

Histology
Tissues were fixed in 10% zinc formalin, then processed for paraffin sectioning (5-μm sections), and stained with hematoxylin and eosin. Anti-F4/80 (MCA497R; AbD Serotec) was used to assess macrophage infiltration in the liver.

Statistical Analysis

Data are presented as means ± SEM. Differences between groups were tested using one-way ANOVA and post hoc Tukey test, with significance accepted at $P < 0.05$.

RESULTS

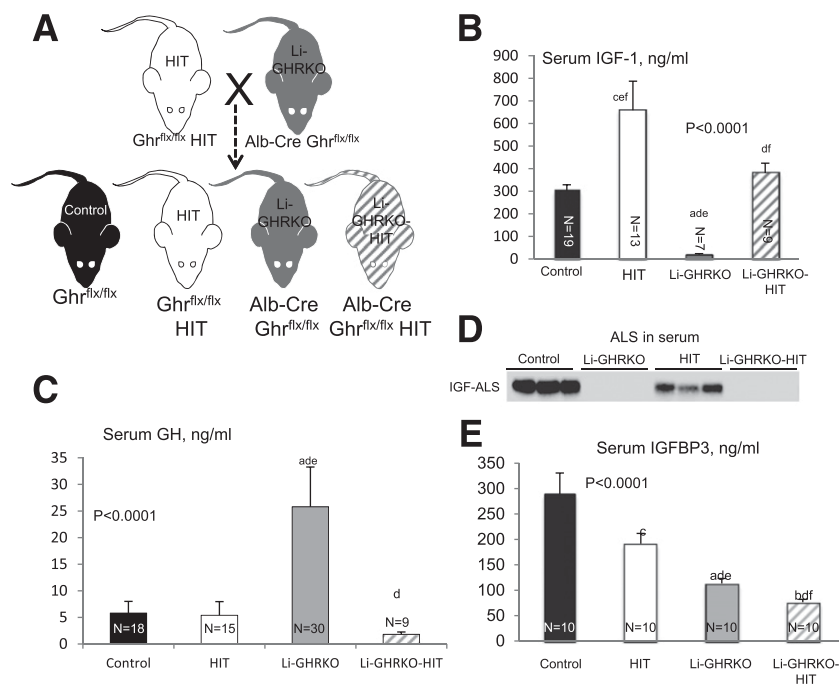### Restoration of Hepatic IGF-1 in the Li-GHRKO Mice

To restore IGF-1 in the liver-specific GHRKO mice, we crossed the Li-GHRKO mice with the HIT mice (27) (Fig. 1A), in which the rat IGF-1 transgene expressed specifically in liver under the transthyretin promoter.

Ghr gene ablation in liver resulted in ~95% reductions in serum IGF-1 in Li-GHRKO mice (Fig. 1B), whereas expression of the *Igf-1* transgene in the HIT mice increased serum IGF-1 levels by approximately twofold. Crossing of the Li-GHRKO and HIT mice normalized serum IGF-1 levels (in Li-GHRKO-HIT). Serum GH levels increased fivefold in the Li-GHRKO, whereas restoration of liver IGF-1 (Li-GHRKO-HIT) normalized GH levels (Fig. 1C).

The ALS is a surrogate marker of GHR action in liver. Accordingly, ALS protein levels in serum were undetectable in both Li-GHRKO and Li-GHRKO-HIT mice (Fig. 1D). Serum IGFBP-3 levels reduced significantly in Li-GHRKO and Li-GHRKO-HIT mice (Fig. 1E), likely due to blunted expression of ALS (that stabilizes the IGF-1/IGFBP3 complex in serum) and increased susceptibility of unbound IGFBP-3 to degradation.

IGF-1 Improves Systemic Glucose/Lipid Homeostasis and Body Composition in Li-GHRKO-HIT Mice

Li-GHRKO mice show increased blood glucose, increased serum insulin levels, and severely impaired insulin tolerance tests (Fig. 2). Restoration of hepatic *Igf-1* (Li-GHRKO-HIT mice) normalized the fed and fasting blood glucose (Fig. 2A), insulin (Fig. 2B), and insulin tolerance tests (Fig. 2D). In accordance with a recent study (31) showing that elevated IGFBP-1 improves whole-body insulin sensitivity and glucose tolerance, we found that in the Li-GHRKO-HIT mice serum IGFBP-1 increased fivefold (Fig. 2E), suggesting that it may play a role in the improvement of overall insulin sensitivity. A previous study using the Li-GHRKO mice (32) showed that IGFBP-1 levels increased by 2.5-fold despite elevated levels of its inhibitor insulin. This may be in part due to hepatic insulin resistance, progressive hepatic steatosis (33), or, alternatively, a compensatory response to significant reductions in IGFBP-3. Our results differ from those previously reported (22), in which administration of recombinant human (rh)IGF-1 via osmotic pump into the Li-GHRKO mice did not correct the metabolic phenotype. We have previously shown that in the absence of ALS, the half-life of rhIGF-1 is very short, and it is rapidly cleared from circulation (34). Thus, infusing rhIGF-1 via osmotic pumps for a relatively short time (4 weeks) to Li-GHRKO mice with already severe hepatic steatosis is inefficient.

Figure 1—Restoration of hepatic IGF-1 gene expression in Li-GHRKO mice. *A*: HIT were crossed with Li-GHRKO mice to yield the following groups: control mice harbored the floxed *ghr* gene, HIT mice harbored the rat IGF-1 transgene and floxed *ghr* gene, Li-GHRKO harbored the floxed *ghr* gene and albumin (Alb) promoter–derived Cre transgene, and the Li-GHRKO-HIT mice harbored the floxed *ghr* gene, albumin promoter–derived Cre transgene, and HIT. *B*: Serum IGF-1 levels in male mice at 16 weeks of age. *C*: Serum GH levels in male mice at 8–16 weeks of age. *D*: Serum ALS levels of 16-week-old male mice. *E*: Serum IGFBP-3 in male mice at 16 weeks of age. Data presented as mean ± SEM. *N* indicates sample size. Significance accepted at $P < 0.05$: control vs. Li-GHRKO (a), control vs. Li-GHRKO-HIT (b), control vs. HIT (c), Li-GHRKO vs. Li-GHRKO-HIT (d), Li-GHRKO vs. HIT (e), and Li-GHRKO-HIT vs. HIT (f).
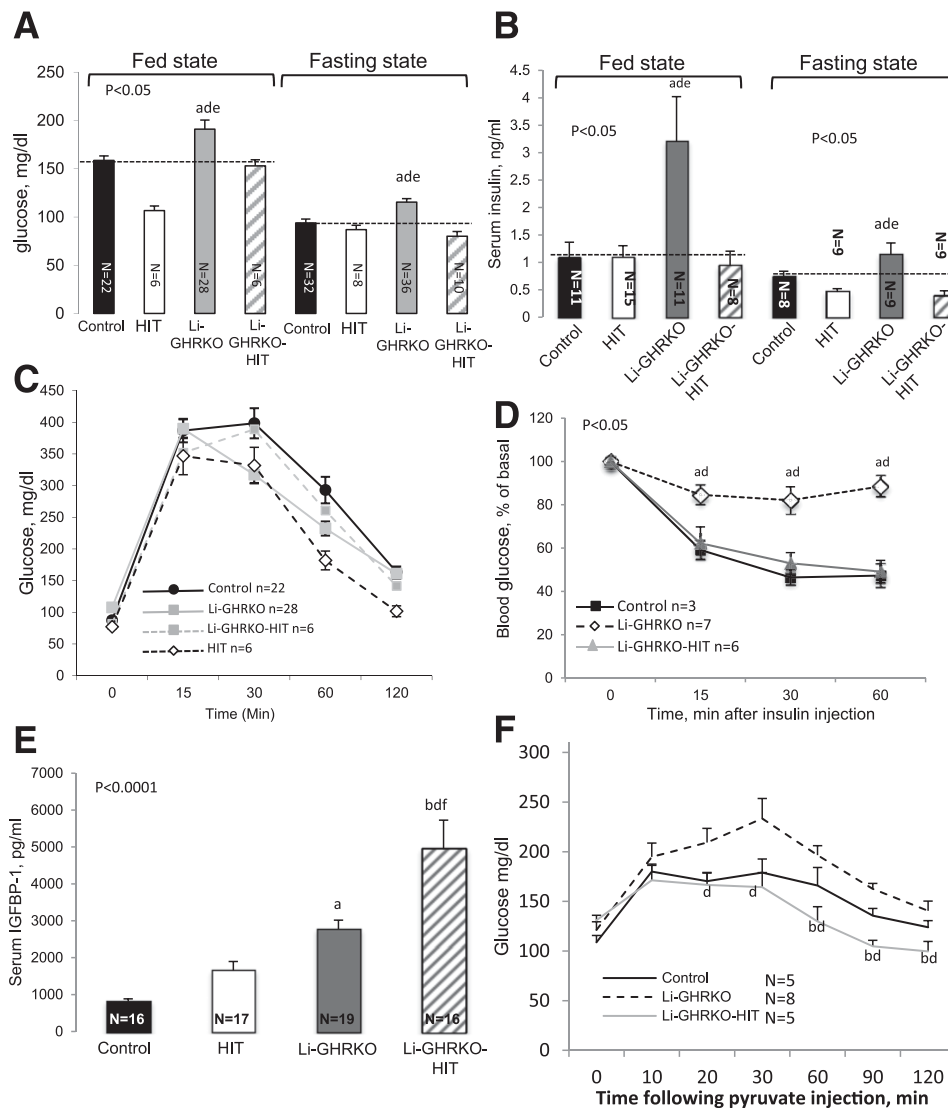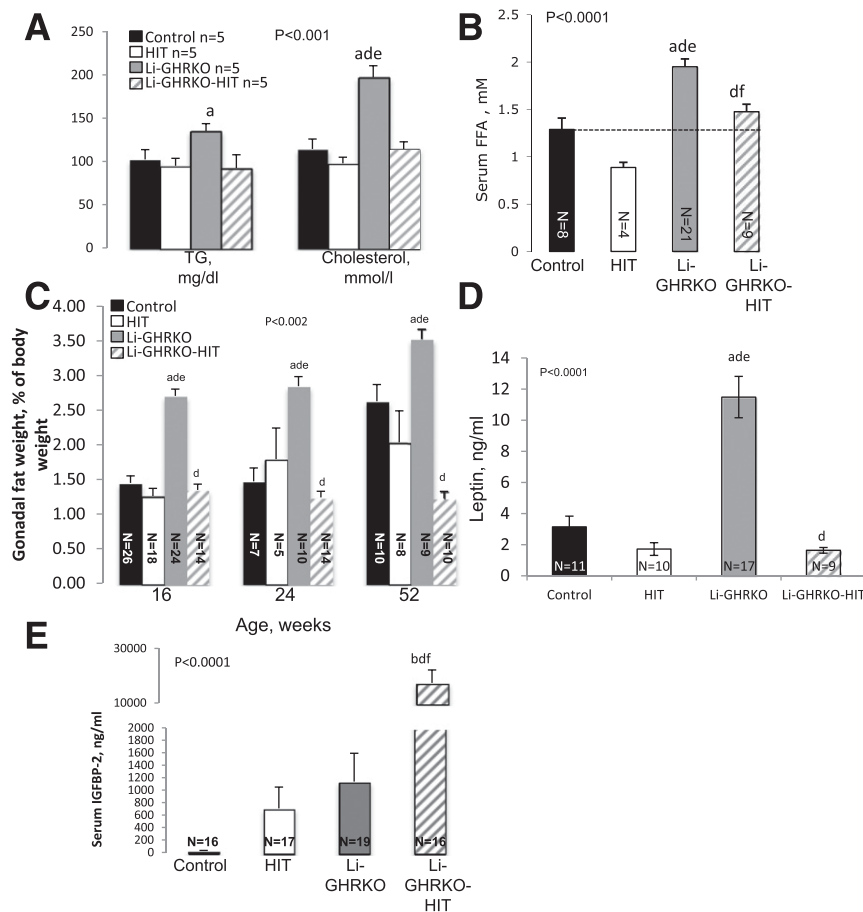
Figure 2—Hepatic-derived IGF-1 improves systemic glucose homeostasis in the Li-GHRKO mice. Blood glucose levels (*A*) and serum insulin levels (*B*) were determined in male mice at 16 weeks of age. Intraperitoneal glucose tolerance test (*C*) and intraperitoneal insulin tolerance test (*D*) performed in 16- to 20-week-old male mice in the fed state. *E*: Serum IGFBP-1 levels determined in male mice at 16–24 weeks of age. *F*: iPTT performed in 16- to 20-week-old male mice. Data presented as mean ± SEM. *N* indicates sample size. Significance accepted at *P* < 0.05: control vs. Li-GHRKO (a), control vs. Li-GHRKO-HIT (b), Li-GHRKO vs. Li-GHRKO-HIT (d), Li-GHRKO vs. HIT (e), and Li-GHRKO-HIT vs. HIT (f).

In view of the improved whole-body insulin sensitivity (suggesting improved muscle insulin sensitivity), we performed an intraperitoneal pyruvate tolerance test (iPTT) to examine whether hepatic insulin sensitivity was also improved in Li-GHRKO-HIT mice. We found significant improvement in iPTT in Li-GHRKO-HIT as compared with Li-GHRKO mice, suggesting that part of whole-body improvement in insulin sensitivity was also due to decreased hepatic glucose production (HGP) (Fig. 2*F*).

Lipid profile in serum revealed significant increases in TG and cholesterol (Fig. 3*A*) and serum FFA levels (Fig. 3*B*) in the Li-GHRKO mice, which were normalized in Li-GHRKO-HIT mice, suggesting that increases in hepatic-derived IGF-1 can override the impaired systemic glucose and lipid metabolism resulting from GHR resistance in the liver.

Insulin resistance in the Li-GHRKO mice associated with changes in body composition. Body weight was not affected in Li-GHRKO or the Li-GHRKO-HIT mice (Supplementary Fig. 1*A*). However, we detected an approximate twofold increase in the weights of several fat pads in Li-GHRKO (Fig. 3*C*), which correlated with increases in serum leptin levels (Fig. 3*D*). With age (at 52 weeks), control mice showed increases in body adiposity, resulting in a difference of only 25% between Li-GHRKO and control mice. Hepatic-derived *Igf-1* in Li-GHRKO-HIT mice brought body adiposity (Fig. 3*C*) and serum leptin (Fig. 3*D*) to normal levels. A previous study (34) has demonstrated that leptin regulates IGFBP-2, which in turn improves glucose metabolism and hepatic insulin sensitivity by suppressing HGP and gene expression of enzymes involved

Figure 3—Hepatic-derived IGF-1 improves systemic lipid homeostasis and body composition in the Li-GHRKO mice. *A*: Serum TG and cholesterol in males at 16 weeks of age. *B*: Serum FFAs in the fed state in males at 16 weeks of age. *C*: Relative gonadal fat pad wet-weight to body weight at the indicated ages. *D*: Serum leptin levels in males at 16 weeks of age. *E*: Serum IGFBP-2 levels in males at 16–24 weeks of age. Data presented as mean ± SEM. *N* indicates sample size. Significance accepted at *P* < 0.05: control vs. Li-GHRKO (a), control vs. Li-GHRKO-HIT (b), Li-GHRKO vs. Li-GHRKO-HIT (d), Li-GHRKO vs. HIT (e), and Li-GHRKO-HIT vs. HIT (f).

in gluconeogenesis and FA synthesis. We found that serum IGFBP-2 levels increased >10-fold in the Li-GHRKO-HIT mice (Fig. 3*E*), which may explain in part the improvement in overall insulin sensitivity in those mice.

IGF-1 Is Insufficient to Restore Lipid Metabolism in the Livers of GH-Resistant Mice

Relative liver weight in the Li-GHRKO mice increased at all ages and was reduced in the Li-GHRKO-HIT mice (Fig. 4*A*). Li-GHRKO mice exhibited steatotic livers by histology (Fig. 4*B*) and showed an approximately sixfold increase in liver TG content (Fig. 4*C*) and FA content detected by GC/MS (Fig. 4*D* and Supplementary Table 1). Hepatic steatosis persisted even after restoration of liver *Igf-1* (Li-GHRKO-HIT mice), although to a lesser degree (Fig. 4*B*).

In accordance with previous findings with mutated GHR and liver-specific STAT5 knockout (35) mice showing a negative regulation of the FA translocase CD36 by STAT5, we found significantly increased CD36 expression in both Li-GHRKO and the Li-GHRKO-HIT mice (Fig. 5*A*). Likewise, the FA transport proteins 2 and 5 and the LDL receptor that regulates cholesterol metabolism increased in the

Li-GHRKO and Li-GHRKO-HIT mice (Fig. 5*A*), suggesting increased hepatic lipid uptake in the absence of GHR. Further, we found that liver content of linoleic and docosahexaenoic acids, which are not synthesized de novo and must be taken up by hepatocytes, are increased in Li-GHRKO mice (Supplementary Table 1). Although the levels of hepatic linoleic acid were reduced in Li-GHRKO-HIT when compared with Li-GHRKO mice, they were not normalized. In an attempt to decrease GH-mediated lipolysis in fat, we deleted the GHR in fat of the Li-GHRKO-HIT mice using the adiponectin-driven cre-transgenic mice. We show that despite normalization of serum GH, IGF-1, and insulin, as well as inactivation of the GHR in fat, hepatic lipid content in the Li/Fat-GHRKO-HIT mice was not normalized (Supplementary Fig. 1*B*). Overall, the data suggest that GHR in liver controls lipid uptake independent of IGF-1 or insulin.

Gene expression of stearoyl-CoA desaturase-1 (SCD-1), the rate-limiting enzyme that converts the palmitate (16:0) and stearate (18:0) to palmitoleate (16:1n7) and oleate (18:1n9), respectively, increased significantly in both Li-GHRKO and the Li-GHRKO-HIT mice, suggesting
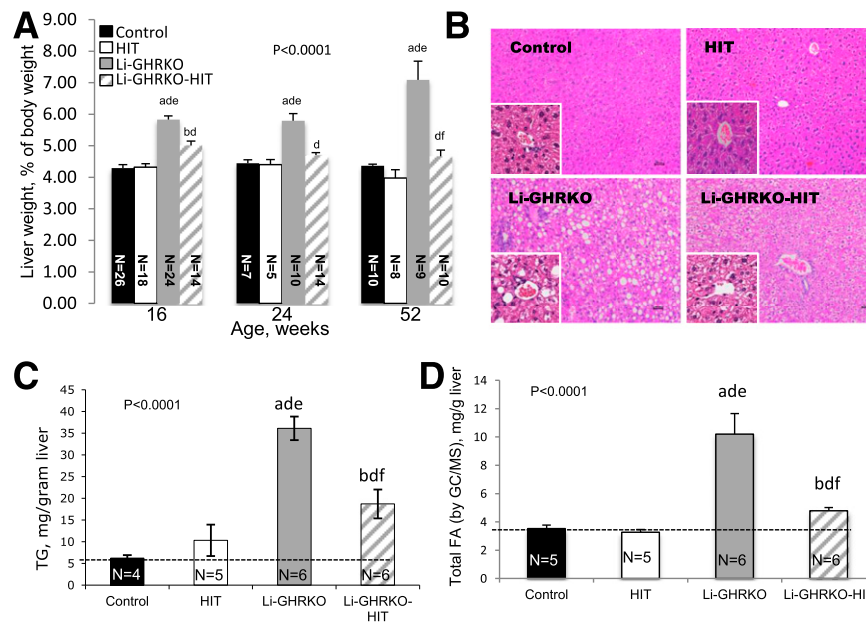
Figure 4—Hepatic *Igf-1* transgene does not resolve hepatic steatosis in the Li-GHRKO mice. *A*: Relative liver wet-weight to body weight was followed in several age groups as indicated. *B*: Hematoxylin/eosin staining of liver sections from 16-week-old control, Li-GHRKO, HIT, and Li-GHRKO-HIT mice. Scale bars = 100 μm. *C*: Hepatic TG content. *D*: Hepatic FA content in 16-week-old male mice measured by GC/MS. Data presented as mean ± SEM. *N* indicates sample size. Significance accepted at *P* < 0.05: control vs. Li-GHRKO (a), control vs. Li-GHRKO-HIT (b), Li-GHRKO vs. Li-GHRKO-HIT (d), Li-GHRKO vs. HIT (e), and Li-GHRKO-HIT vs. HIT (f).

an increase in de novo lipogenesis (DNL) (Fig. 5*B*). In accordance with previous publications (36,37), we show that the SCD-1 index (the ratio of 18:1/18:0 by GC/MS) increased threefold in the Li-GHRKO mice (Fig. 5*C* and Supplementary Table 1), suggesting an increased DNL. Li-GHRKO-HIT showed a significant decrease in SCD-1 index as compared with the Li-GHRKO mice, but this was still significantly higher than controls, suggesting that hepatic IGF-1 improved but did not resolve DNL in the absence of GHR. Increased DNL correlated with increased gene expression of the sterol regulatory element-binding protein 1, acetyl-CoA carboxylase, and FA synthase (Fig. 5*B*) in Li-GHRKO and the Li-GHRKO-HIT mice. Finally, carnitine palmitoyl-transferase 1 (CPT-1) and peroxisome proliferator–activated receptor-γ coactivator 1α increased in Li-GHRKO and the Li-GHRKO-HIT mice, suggesting increased FA oxidation.

Compromised hepatic lipid metabolism in Li-GHRKO and the Li-GHRKO-HIT mice was associated with impaired glucose metabolism (Fig. 5*D*). Gene expression of the GLUT2 and glucokinase increased in Li-GHRKO mice, indicating enhanced glucose flux. Pyruvate carboxylase (PC), PCK1/PEPCK, and glucose 6 phosphatase, which are critical enzymes for gluconeogenesis, were also elevated in livers of Li-GHRKO. Despite significant improvement in iPTT in Li-GHRKO-HIT mice, expression of these genes was still elevated. Expression of genes involved in glycogen synthesis was highly variable (Supplementary Fig. 1*C*). However, we found significant increases in hepatic glycogen content in Li-GHRKO mice (Fig. 5*E*), which is in agreement with studies in humans showing that in states of hyperinsulinemia

with hyperglycemia (Li-GHRKO mice), hepatic glycogen synthesis is maximized (38). Improvement in insulin sensitivity associated with decreased glycogen content in the livers of the Li-GHRKO-HIT mice (Fig. 5*E*).

IGF-1 Modulates Oxidative Stress, but Is Insufficient to Resolve Liver Inflammation in GH-Resistant Mice

Liver expression of glutathione peroxidase, superoxide dismutase (SOD), catalase 2, and the nuclear factor erythroid 2–related factor-2 increased significantly in Li-GHRKO and Li-GHRKO-HIT mice (Fig. 6*A*). Protein carbonylation (oxidatively damaged proteins) in the liver did not differ between the groups (Fig. 6*B*). However, Li-GHRKO mice showed significantly increased levels of oxidized lipids in liver (Fig. 6*C*) and serum (Fig. 6*D*) that were normalized in the Li-GHRKO-HIT mice. Because adult hepatocytes express very low levels of the IGF-1 receptor, we postulated that IGF-1 elicited its effects on lipid peroxidation via its actions on hepatic stellate cells or via the IR on hepatocytes. We found that IR levels increased significantly in livers of Li-GHRKO-HIT as compared with Li-GHRKO mice (Supplementary Fig. 1*D*), suggesting that hepatic-derived IGF-1 may act locally via the IR to reduce oxidative stress in liver. Hepatic steatosis in the Li-GHRKO mice associated with liver injury as indicated by elevated levels of AST and ALT (Fig. 6*E*) and elevated lipid peroxidation (Fig. 6*C*) that were normalized with hepatic-IGF-1. Note that muscle protein carbonylation (Supplementary Fig. 1*E*) and the levels of oxidized lipids (Supplementary Fig. 1*F*) reduced in Li-GHRKO-HIT mice and may contribute to overall improved insulin sensitivity.
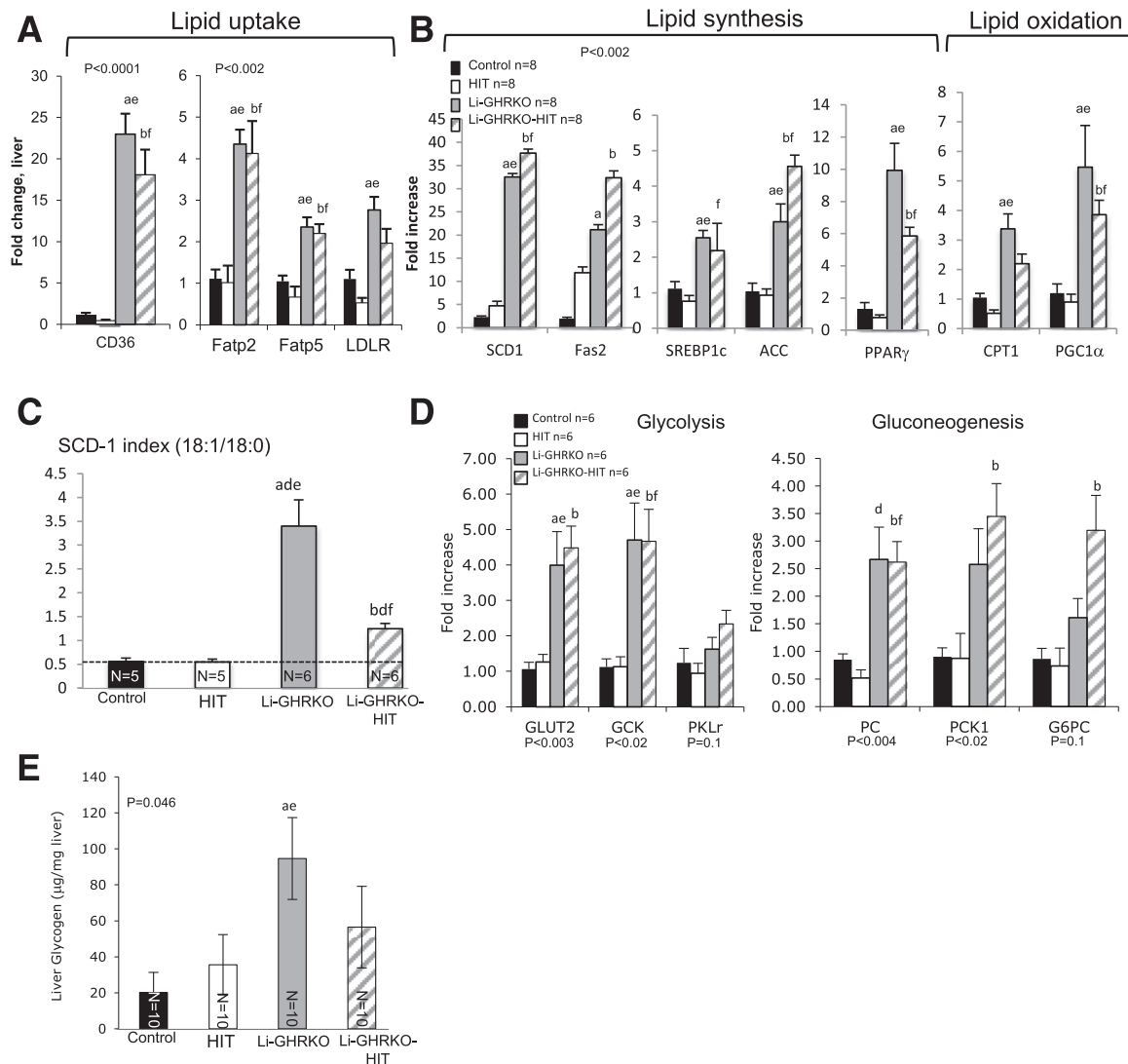
Figure 5—Hepatic *Igf-1* transgene does not resolve hepatic lipid metabolism in Li-GHRKO mice. *A* and *B*: Liver gene expression of key players in lipid metabolism was determined by real-time PCR ($n = 8$/genotype). *C*: SCD-1 index determined by the ratio of hepatic stearic and oleic acid concentrations determined by GC/MS. *D*: Hepatic gene expression of key players in glycolysis (GLUT2, glucokinase [GCK], and liver pyruvate kinase [PKLr]) and gluconeogenesis (PC, PCK1, and glucose 6 phosphatase [G6PC]). Liver RNA extracted from 16- to 24-week-old male mice and processed for real-time PCR assay. *E*: Hepatic glycogen content assayed in livers of 16-week-old male mice. Data presented as mean ± SEM. *N* indicates sample size. Significance accepted at $P < 0.05$: control vs. Li-GHRKO (a), control vs. Li-GHRKO-HIT (b), Li-GHRKO vs. Li-GHRKO-HIT (d), Li-GHRKO vs. HIT (e), and Li-GHRKO-HIT vs. HIT (f). ACC, acetyl-CoA carboxylase; Fas2, FA synthase 2; Fatp, FA transport protein; LDLR, LDL receptor; PGC1α, peroxisome proliferator–activated receptor-γ coactivator 1α; PPARγ, peroxisome proliferator–activated receptor γ; SREBP1c, sterol regulatory element–binding protein 1c.

Livers of Li-GHRKO and Li-GHRKO-HIT mice showed significantly more F4/80-positive cells (Fig. 7A), increased F4/80 protein levels (Fig. 7B), and increased expression of *f4/80* (Fig. 7C) and monocyte chemoattractant protein-1 (*mcp1*), both markers of macrophages. Expression of the inflammatory cytokines tumor necrosis factor-α (TNF-α), interleukin (IL)-1β, IL-6, and IL-18 increased in livers of Li-GHRKO and Li-GHRKO-HIT mice (Fig. 7C). The pathogenesis of NAFLD associates with increased Toll-like receptor and its adaptor protein MyD88 (39), which both increased in livers of Li-GHRKO and Li-GHRKO-HIT mice. Lastly, the chemokine RANTES (CCL5), implicated in the progression of hepatic inflammation (40),

also increased in livers of Li-GHRKO and Li-GHRKO-HIT mice. Note that infiltration of T cells was not evident histologically or by CD4/CD8 gene expression. Serum levels of IL-6 and TNF-α did not reflect the gene expression patterns (Fig. 7D). IL-6 levels increased only in serum of the HIT mice, whereas serum TNF-α was similar between the groups, suggesting that GH resistance–induced steatosis in the adult mouse results in inflammatory response that at young adulthood is localized to the liver.

DISCUSSION

We have created a new mouse model to dissect the effects of GHR signaling in liver metabolism in which we excluded
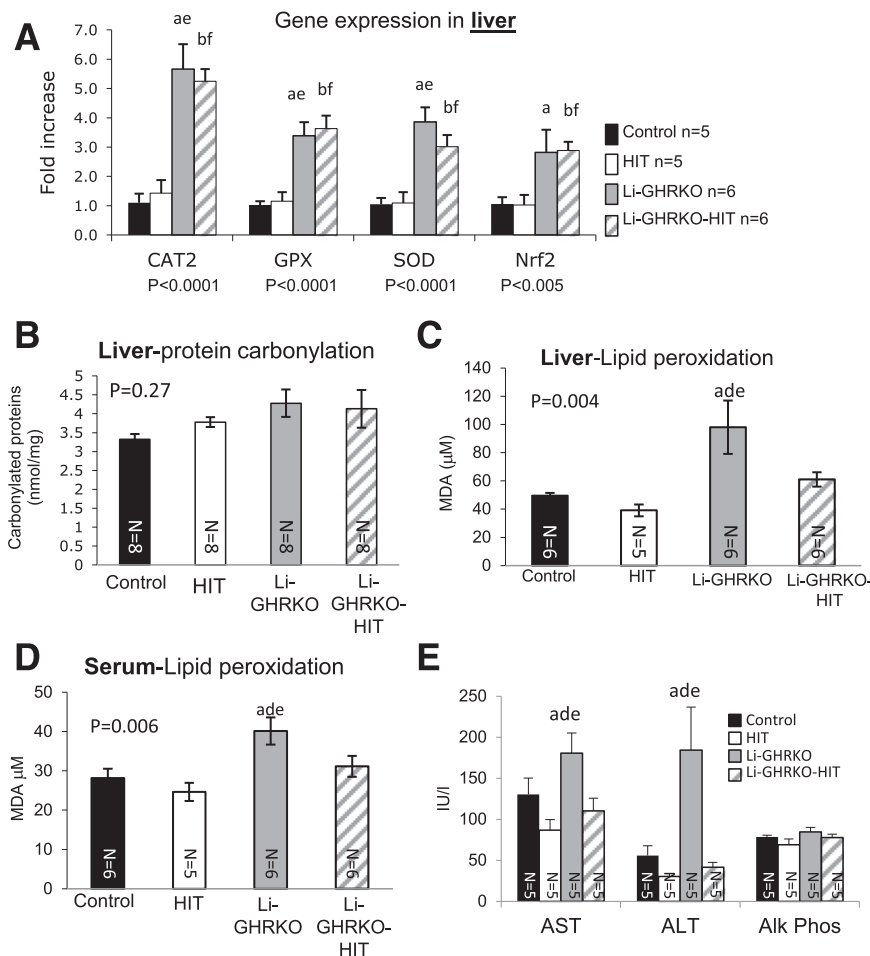
Figure 6—Hepatic IGF-1 modulates oxidative stress in liver and serum. *A*: Liver gene expression of enzymes involved in oxidative stress response in males at 16 weeks measured by real-time PCR. *B*: Protein carbonylation was determined using a spectrophotometric assay of liver protein extracts from male mice at 24 weeks of age. Lipid peroxidation measured using thiobarbituric acid–reactive substances assay in liver (*C*) and serum (*D*) from male mice at 24 weeks of age. *E*: Serum levels of AST, ALT, and alkaline phosphatase (Alk Phos) in males at 16 weeks of age. Data presented as mean $\pm$ SEM. *N* indicates sample size. Significance accepted at *P* < 0.05: control vs. Li-GHRKO (a), control vs. Li-GHRKO-HIT (b), Li-GHRKO vs. Li-GHRKO-HIT (d), Li-GHRKO vs. HIT (e), and Li-GHRKO-HIT vs. HIT (f). CAT2, catalase 2; GPX, glutathione peroxidase; MDA, malondialdehyde; Nrf2, nuclear factor erythroid 2–related factor-2.

the possible contribution of concomitant reductions in IGF-1 to the overall phenotype. Our study clearly indicates that restoration of IGF-1 in the context of hepatic GH resistance normalized whole-body insulin sensitivity and serum lipid profile in the adult mouse (16–24 weeks), a phenotype that persisted to 52 weeks of age. However, IGF-1 did not resolve hepatic steatosis, as enhanced hepatic lipid uptake and DNL were still evident. Importantly, IGF-1 was insufficient for protecting against steatosis-induced hepatic inflammation.

Li-GHRKO and liver-specific IGF-1–deficient (LID) mice, with high levels of GH show insulin resistance (41). Hepatic production of IGF-1 (Li-GHRKO-HIT) rescued overall insulin sensitivity likely via normalization of serum GH levels and improved muscle insulin responsiveness. Improvement in overall insulin sensitivity in the Li-GHRKO-HIT mice associated also with normalized iPTT, suggesting partial improvement in hepatic insulin sensitivity. IGFBP-1, a

surrogate marker of insulin resistance, was elevated in the Li-GHRKO-HIT mice and may also contribute to the improvement in whole-body insulin sensitivity. Li-GHRKO-HIT mice also showed improved lipid profile in serum and normalized body adiposity that correlated with normalized serum leptin levels and >10-fold increase in IGFBP-2 levels that were previously shown to enhance insulin sensitivity (34). At this point, improvement in whole-body insulin sensitivity together with normalized leptin levels in the Li-GHRKO-HIT mice most likely involves central (neuroendocrine) regulation, which controls body composition via leptin-dependent and -independent mechanisms.

The contribution of GH to body adiposity is documented in both humans and mice. Patients with Laron syndrome (42), GH-deficient subjects (43), and GHRKO mice exhibit increases in body adiposity (44), whereas patients with acromegaly (45) and the bovine GH-transgenic mice are lean (46). Together with the documented lipolytic
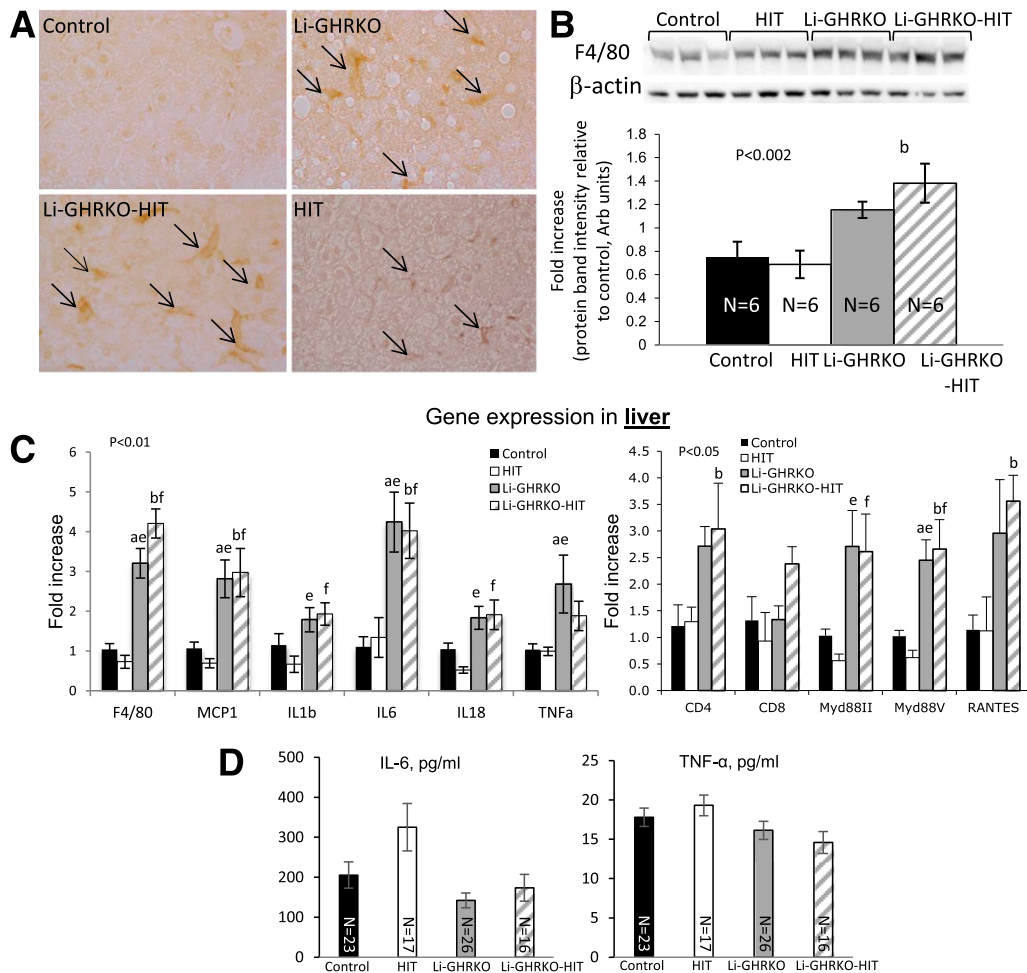
Figure 7—Hepatic IGF-1 modulates oxidative stress in liver and serum but is insufficient to resolve liver inflammation in the Li-GHRKO mice. *A*: Liver sections from 16-week-old mice immunostained with anti-F4/80 antibody; arrows indicate F4/80-positive cells. *B*: F4/80 protein levels assessed by Western immunoblotting in 16-week-old mice. *C*: Liver gene expression of inflammatory markers (*n* = 6/genotype). *D*: Serum levels of IL-6 and TNF-α at 16–24 weeks of age. Data presented as mean ± SEM. *N* indicates sample size. Significance accepted at *P* < 0.05: control vs. Li-GHRKO (a), control vs. Li-GHRKO-HIT (b), Li-GHRKO vs. HIT (e), and Li-GHRKO-HIT vs. HIT (f).

effects of GH, it is suggested that GH-mediated lipolysis leads to reductions in fat mass. Nonetheless, the Li-GHRKO and LID mouse models, which show high levels of GH, exhibit increased body adiposity, suggesting a more complex regulatory mechanism that may involve central regulatory pathways in the hypothalamus. Our studies indicate that the insulin resistance in LID (41) and Li-GHRKO mice contributes to the enhanced body adiposity. When serum IGF-1 was restored (Li-GHRKO-HIT), insulin sensitivity improved and resulted in decreased body adiposity.

Despite overall improved body composition and insulin responsiveness in the Li-GHRKO-HIT mice, hepatic insulin resistance was not completely resolved. Previous reports have shown that augmented HGP (gluconeogenesis) in states of insulin resistance (31) associates with increased expression of PC and PEPCK, as seen in Li-GHRKO and Li-GHRKO-HIT mice, although in the latter, iPTT (which indicates improved liver responsiveness to insulin) improved,

and the insulin resistance was insufficient to cause hyperglycemia. We also found increases in glycogen content in livers of the Li-GHRKO that manifest systemic insulin resistance, whereas glycogen content in livers of Li-GHRKO-HIT mice was comparable to normal, suggesting an improved (but likely unresolved) insulin sensitivity in the latter.

In cases of GH resistance, the increase in liver TG content may be due to secondary effects of GH-mediated lipolysis in white adipose tissue. However, ablation of JAK2 both in liver and adipose tissue resulted in significant reductions in hepatic TG levels as compared with JAK2L mice (23), but was still ~2.5-fold greater than controls. Ablation of CD36 in the JAK2L mice (DKO-JAK2/CD36) improved hepatic TG content (5) as compared with JAK2L, but was still ~20-fold higher than control mice. We found increases in CD36 gene expression in Li-GHRKO and Li-GHRKO-HIT mice that correlated with hepatic increases in the levels of linoleic and docosahexaenoic acids, which

are not synthesized de novo, suggesting increased lipid uptake. Hepatic IGF-1 significantly reduced the levels of these acids (Li-GHRKO-HIT) but not to normal levels. Further, ablation of GHR in both liver and adipose tissue (liver/fat-GHRKO-HIT mice) did not resolved hepatic steatosis, despite normal levels of blood glucose and insulin, again suggesting that an increase in white adipose tissue lipolysis is not the only cause for hepatic lipid accumulation in states of GH resistance.

On the basis of the theory of Li et al. (47), fatty liver can become resistant to insulin-mediated suppression of HGP, but remains sensitive to insulin-mediated stimulation of lipogenesis. In the Li-GHRKO-HIT mice, despite normal insulin levels and iPTT, hepatic steatosis remained, suggesting that lipid synthesis in livers of these mice is independent of insulin signaling and most likely relates to ablation of the GHR. Our data are also supported by Vatner et al. (48), who showed that the rate of hepatic TG production depends on the rate of FA uptake, is independent of hepatic insulin signaling, and, with clinical data showing that low levels of circulating IGF-1 may have a role in the development of NAFLD, is independent of insulin resistance. Accordingly, we note that the high levels of insulin found in the LID mice did not lead to hepatic steatosis (15,41), suggesting that increased hepatic lipid synthesis in the Li-GHRKO mice relates directly to the

ablation of GHR action in liver. Consequently, we detected increases in SCD-1 gene expression and SCD-1 index in the Li-GHRKO and Li-GHRKO-HIT mice, suggesting that hepatic GHR regulates liver DNL independent of IGF-1. Notably, in the Li-GHRKO-HIT mice, SCD-1 index was reduced but not normalized, suggesting that GHR signaling directly suppresses hepatic DNL. These data are in agreement with previous study showing a twofold increase in DNL in GH-resistant mice (49). Overall, it is postulated that both lipid uptake and DNL occur in states of hepatic GH resistance independent of IGF-1.

Excess lipid storage in the liver leads to enhanced β-oxidation of FFAs, which is regulated by CPT-1. Li-GHRKO and Li-GHRKO-HIT mice show increases in CPT-1 gene expression, suggesting increases in β-oxidation. Increased β-oxidation results in overproduction of reactive oxygen species (ROS), eventually leading to mitochondrial dysfunction. Oxidation of lipids by extramitochondrial oxidation systems, such as microsomal and peroxisomal oxidation, also leads to increased ROS production (40). Accumulation of ROS and nitrogen species is a hallmark of NAFLD (26). We found increases in lipids peroxidation in the Li-GHRKO mice in serum and liver, which was restored to normal by hepatic IGF-1 (Li-GHRKO-HIT mice). Despite improvement in lipid peroxidation, an increase in oxidative stress may still be occurring in the
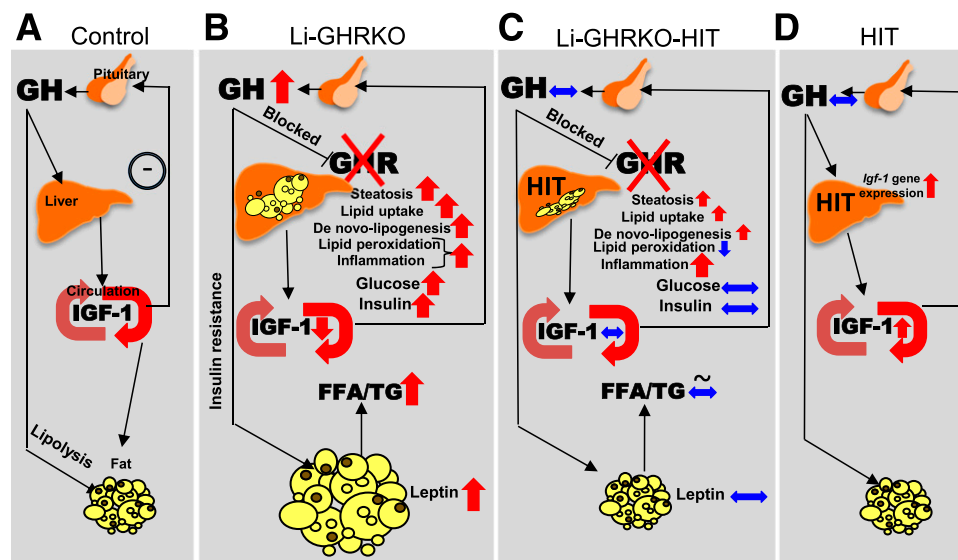
Figure 8—IGF-1–independent effects of GHR in liver involve mainly DNL. A: In control animals, GH, secreted from the pituitary, promotes liver production and secretion of IGF-1 that is delivered to tissues via circulation. IGF-1 feeds back negatively on GH secretion. B: Ablation of GHR in liver (Li-GHRKO) results in significant reductions in liver IGF-1 production and elevations in GH secretion. Increased GH levels contribute to overall increased insulin resistance (reflected by high levels of serum insulin and elevated blood glucose) and increased body adiposity (evident by increased circulating leptin levels). Li-GHRKO mice show severe hepatic steatosis, resulting from increased DNL and increased lipid uptake. The impaired lipid metabolism in the Li-GHRKO mice associates with protein and lipid oxidation in liver, as well as inflammation in the liver. C: Restoration of hepatic IGF-1 in the Li-GHRKO-HIT mice normalizes serum IGF-1 and GH secretion. This associates with reduction in body adiposity and serum leptin and normalization of serum lipids, blood glucose, and serum insulin levels. Hepatic steatosis in Li-GHRKO-HIT mice reduced as compared with Li-GHRKO mice but was not resolved. Expression levels of genes involved in DNL and lipid uptake were increased to levels comparable to those in Li-GHRKO mice. Liver inflammation was high and did not resolve with hepatic IGF-1. D: Lastly, the HIT mice express the IGF-1 transgene in liver and exhibit twofold increase in serum IGF-1. HIT mice show normal levels of serum GH and insulin during young adulthood.

Li-GHRKO-HIT liver because we found significant increases in SOD and catalase in both Li-GHRKO and Li-GHRKO-HIT mice.

NAFLD associates with low-grade inflammation, which often proceeds to chronic inflammation (7). Kupffer cells are liver-resident macrophages that show high levels of the cell-surface marker F4/80. Activated Kupffer cells produce proinflammatory cytokines such as IL-1β and TNF-α and secrete chemokines to recruit blood-derived monocytes/macrophages into the liver and play key roles in the initiation and progression of liver inflammation (50). Indeed, we found increases in F4/80 and MCP-1 in both Li-GHRKO and Li-GHRKO-HIT mice, which associated with increased expression of MyD88, RANTES (CCL5), IL-6, IL-1β, and TNF-α. Serum levels of IL-1β and TNF-α at 16–24 weeks did not differ from controls, but during advanced adulthood (1 and 2 years), they increased in both Li-GHRKO and Li-GHRKO-HIT mice (data not shown).

In summary, we have shown that hepatic GH resistance associates with overall impaired lipid metabolism, insulin resistance, and increased body adiposity. Hepatic lipid accumulation in states of chronic GH resistance results from increased lipid uptake and increased DNL, indicating that GH directly regulates these processes in the liver. The impaired lipid metabolism, along with severe hepatic insulin resistance, leads to overall increased oxidative stress and initiates inflammation (Fig. 8). Restoration of hepatic IGF-1 (Li-GHRKO-HIT) resolved overall insulin resistance and partially alleviated hepatic oxidative stress, but did not resolve hepatic steatosis or inflammation.

Author Contributions. Z.L. conducted the experiments. J.C.-C. and R.D.K. measured FA composition by GC/MS. B.N.C. conducted liver histology and serum lipid profiles. R.M. and Z.G. conducted liver protein carbonylation assay. H.W. conducted liver histology and serum lipid profiles and helped in experimental design and discussion. S.Y. designed the experiments and wrote the paper. S.Y. is the guarantor of this work and, as such, had full access to all the data in the study and takes responsibility for the integrity of the data and the accuracy of the data analysis.

References

1. Browning JD, Szczepaniak LS, Dobbins R, et al. Prevalence of hepatic steatosis in an urban population in the United States: impact of ethnicity. Hepatology 2004;40:1387–1395

2. Xu L, Xu C, Yu C, et al. Association between serum growth hormone levels and nonalcoholic fatty liver disease: a cross-sectional study. PLoS One 2012;7:e44136

3. Chen QR, Braun R, Hu Y, et al. Multi-SNP analysis of GWAS data identifies pathways associated with nonalcoholic fatty liver disease. PLoS One 2013;8:e65982

4. Laron Z, Ginsberg S, Webb M. Nonalcoholic fatty liver in patients with Laron syndrome and GH gene deletion - preliminary report. Growth Horm IGF Res 2008; 18:434–438

5. Hazlehurst JM, Tomlinson JW. Non-alcoholic fatty liver disease in common endocrine disorders. Eur J Endocrinol 2013;169:R27–R37

6. Arturi F, Succurro E, Procopio C, et al. Nonalcoholic fatty liver disease is associated with low circulating levels of insulin-like growth factor-I. J Clin Endocrinol Metab 2011;96:E1640–E1644

7. Fusco A, Miele L, D'Uonnolo A, et al. Nonalcoholic fatty liver disease is associated with increased GHBP and reduced GH/IGF-I levels. Clin Endocrinol (Oxf) 2012;77:531–536

8. Sumida Y, Yonei Y, Tanaka S, et al. Lower levels of insulin-like growth factor-1 standard deviation score are associated with histological severity of non-alcoholic fatty liver disease. Hepatol Res 2015;45:771–781

9. Völzke H, Nauck M, Rettig R, et al. Association between hepatic steatosis and serum IGF1 and IGFBP-3 levels in a population-based sample. Eur J Endocrinol 2009;161:705–713

10. Huang L, Steyn FJ, Tan HY, et al. The decline in pulsatile GH secretion throughout early adulthood in mice is exacerbated by dietary-induced weight gain. Endocrinology 2012;153:4380–4388

11. Iranmanesh A, Lizarralde G, Veldhuis JD. Age and relative adiposity are specific negative determinants of the frequency and amplitude of growth hormone (GH) secretory bursts and the half-life of endogenous GH in healthy men. J Clin Endocrinol Metab 1991;73:1081–1088

12. Dichtel LE, Yuen KC, Bredella MA, et al. Overweight/Obese adults with pituitary disorders require lower peak growth hormone cutoff values on glucagon stimulation testing to avoid overdiagnosis of growth hormone deficiency. J Clin Endocrinol Metab 2014;99:4712–4719

13. Shalet SM, Toogood A, Rahim A, Brennan BM. The diagnosis of growth hormone deficiency in children and adults. Endocr Rev 1998;19:203–223

14. Bredella MA, Gerweck AV, Lin E, et al. Effects of GH on body composition and cardiovascular risk markers in young men with abdominal obesity. J Clin Endocrinol Metab 2013;98:3864–3872

15. Nishizawa H, Iguchi G, Murawaki A, et al. Nonalcoholic fatty liver disease in adult hypopituitary patients with GH deficiency and the impact of GH replacement therapy. Eur J Endocrinol 2012;167:67–74

16. Takahashi Y, Iida K, Takahashi K, et al. Growth hormone reverses non-alcoholic steatohepatitis in a patient with adult growth hormone deficiency. Gastroenterology 2007;132:938–943

17. Schwarz JM, Mulligan K, Lee J, et al. Effects of recombinant human growth hormone on hepatic lipid and carbohydrate metabolism in HIV-infected patients with fat accumulation. J Clin Endocrinol Metab 2002;87:942

18. Madsen M, Krusenstjerna-Hafstrøm T, Møller L, et al. Fat content in liver and skeletal muscle changes in a reciprocal manner in patients with acromegaly during combination therapy with a somatostatin analog and a GH receptor antagonist: a randomized clinical trial. J Clin Endocrinol Metab 2012;97:1227–1235

19. Steyn FJ, Xie TY, Huang L, et al. Increased adiposity and insulin correlates with the progressive suppression of pulsatile GH secretion during weight gain. J Endocrinol 2013;218:233–244

20. Luque RM, Kineman RD. Impact of obesity on the growth hormone axis: evidence for a direct inhibitory effect of hyperinsulinemia on pituitary function. Endocrinology 2006;147:2754–2763

21. Qin Y, Tian YP. Preventive effects of chronic exogenous growth hormone levels on diet-induced hepatic steatosis in rats. Lipids Health Dis 2010;9:78

22. Fan Y, Menon RK, Cohen P, et al. Liver-specific deletion of the growth hormone receptor reveals essential role of growth hormone signaling in hepatic lipid metabolism. J Biol Chem 2009;284:19937–19944

23. Nordstrom SM, Tran JL, Sos BC, Wagner KU, Weiss EJ. Disruption of JAK2 in adipocytes impairs lipolysis and improves fatty liver in mice with elevated GH. Mol Endocrinol 2013;27:1333–1342

24. Cui Y, Hosui A, Sun R, et al. Loss of signal transducer and activator of transcription 5 leads to hepatosteatosis and impaired liver regeneration. Hepatology 2007;46:504–513

25. List EO, Palmer AJ, Berryman DE, Bower B, Kelder B, Kopchick JJ. Growth hormone improves body composition, fasting blood glucose, glucose tolerance and liver triacylglycerol in a mouse model of diet-induced obesity and type 2 diabetes. Diabetologia 2009;52:1647–1655

26. Yang T, Householder LA, Lubbers ER, et al. Growth hormone receptor antagonist transgenic mice are protected from hyperinsulinemia and glucose intolerance despite obesity when placed on a HF diet. Endocrinology 2015;156: 555–564

27. Wu Y, Sun H, Basta-Pljakic J, et al. Serum IGF-1 is insufficient to restore skeletal size in the total absence of the growth hormone receptor. J Bone Miner Res 2013;28:1575–1586

28. Wu Y, Wang C, Sun H, LeRoith D, Yakar S. High-efficient FLPo deleter mice in C57BL/6J background. PLoS One 2009;4:e8054

29. Yakar S, Liu JL, Stannard B, et al. Normal growth and development in the absence of hepatic insulin-like growth factor I. Proc Natl Acad Sci U S A 1999;96: 7324–7329

30. Kineman RD, Majumdar N, Subbaiah PV, Cordoba-Chacon J. Hepatic PPARγ Is Not Essential for the Rapid Development of Steatosis After Loss of Hepatic GH Signaling, in Adult Male Mice. Endocrinology 2016;157:1728–1735

31. Rajwani A, Ezzat V, Smith J, et al. Increasing circulating IGFBP1 levels improves insulin sensitivity, promotes nitric oxide production, lowers blood pressure, and protects against atherosclerosis. Diabetes 2012;61:915–924

32. List EO, Berryman DE, Funk K, et al. Liver-specific GH receptor gene-disrupted (LiGHRKO) mice have decreased endocrine IGF-I, increased local IGF-I, and altered body size, body composition, and adipokine profiles. Endocrinology 2014;155:1793–1805

33. Li HH, Doiron K, Patterson AD, Gonzalez FJ, Fornace AJ Jr. Identification of serum insulin-like growth factor binding protein 1 as diagnostic biomarker for early-stage alcohol-induced liver disease. J Transl Med 2013;11:266

34. Hedbacker K, Birsoy K, Wysocki RW, et al. Antidiabetic effects of IGFBP2, a leptin-regulated gene. Cell Metab 2010;11:11–22

35. Barclay JL, Nelson CN, Ishikawa M, et al. GH-dependent STAT5 signaling plays an important role in hepatic lipid metabolism. Endocrinology 2011;152: 181–192

36. Lee JJ, Lambert JE, Hovhannisyan Y, et al. Palmitoleic acid is elevated in fatty liver disease and reflects hepatic lipogenesis. Am J Clin Nutr 2015;101:34–43

37. Silbernagel G, Kovarova M, Cegan A, et al. High hepatic SCD1 activity is associated with low liver fat content in healthy subjects under a lipogenic diet. J Clin Endocrinol Metab 2012;97:E2288–E2292

38. Petersen KF, Laurent D, Rothman DL, Cline GW, Shulman GI. Mechanism by which glucose and insulin inhibit net hepatic glycogenolysis in humans. J Clin Invest 1998;101:1203–1209

39. Miura K, Ohnishi H. Role of gut microbiota and Toll-like receptors in non-alcoholic fatty liver disease. World J Gastroenterol 2014;20:7381–7391

40. Bonekamp NA, Völkl A, Fahimi HD, Schrader M. Reactive oxygen species and peroxisomes: struggling for balance. Biofactors 2009;35:346–355

41. Yakar S, Setser J, Zhao H, et al. Inhibition of growth hormone action improves insulin sensitivity in liver IGF-1-deficient mice. J Clin Invest 2004;113:96–105

42. Laron Z. Lessons from 50 Years of Study of Laron Syndrome. Endocr Pract 2015;21:1395–1402

43. Maison P, Griffin S, Nicoue-Beglah M, Haddad N, Balkau B, Chanson P; Metaanalysis of Blinded, Randomized, Placebo-Controlled Trials. Impact of growth hormone (GH) treatment on cardiovascular risk factors in GH-deficient adults: a Metaanalysis of Blinded, Randomized, Placebo-Controlled Trials. J Clin Endocrinol Metab 2004;89:2192–2199

44. Masternak MM, Bartke A, Wang F, et al. Metabolic effects of intra-abdominal fat in GHRKO mice. Aging Cell 2012;11:73–81

45. Freda PU, Shen W, Heymsfield SB, et al. Lower visceral and subcutaneous but higher intermuscular adipose tissue depots in patients with growth hormone and insulin-like growth factor I excess due to acromegaly. J Clin Endocrinol Metab 2008;93:2334–2343

46. Benencia F, Harshman S, Duran-Ortiz S, et al. Male bovine GH transgenic mice have decreased adiposity with an adipose depot-specific increase in immune cell populations. Endocrinology 2015;156:1794–1803

47. Li S, Brown MS, Goldstein JL. Bifurcation of insulin signaling pathway in rat liver: mTORC1 required for stimulation of lipogenesis, but not inhibition of gluconeogenesis. Proc Natl Acad Sci U S A 2010;107:3441–3446

48. Vatner DF, Majumdar SK, Kumashiro N, et al. Insulin-independent regulation of hepatic triglyceride synthesis by fatty acids. Proc Natl Acad Sci U S A 2015; 112:1143–1148

49. Cordoba-Chacon J, Majumdar N, List EO, et al. Growth Hormone Inhibits Hepatic De Novo Lipogenesis in Adult Mice. Diabetes 2015;64:3093–3103

50. Lanthier N. Targeting Kupffer cells in non-alcoholic fatty liver disease/non-alcoholic steatohepatitis: Why and how? World J Hepatol 2015;7:2184–2188